Analysis of a POD-based Approach for Phase and Time Synchronization of Bistatic and Multistatic SAR Systems

Eduardo Rodrigues-Silva and Marc Rodriguez-Cassola
Microwaves and Radar Institute, German Aerospace Centre (DLR), Oberpfaffenhofen, Germany

Abstract

The feasibility of multistatic SAR mission concepts largely relies on the ability to achieve the matching of the carrier phase of the different elements of the constellations to a few degrees. This paper analyses the accuracy of phase synchronization schemes based on precise orbit determination (POD) and GNSS raw data, in which the GNSS receiver and the radar payload share the same oscillator. Performance expressions are contrasted with results from the simulations. The results suggest the proposed approach is capable of delivering reliable estimates of carrier frequency and phase errors in the absence of strong baseline velocity deviations.

1   Introduction

In bistatic and multistatic space radar systems the transmitter and the receiver are spatially separated, which is typically associated with reduced development costs, risks, and enhanced performance. In particular, multistatic constellations allow for lower revisit times and better reconfigurability and scalability. A high revisit time is necessary for applications such as traffic monitoring, risk and disaster management, and security, and such distributed systems could offer a better solution for those applications [1].

In these systems, however, different oscillators are used for modulation and demodulation, and the low-frequency phase errors of the oscillator are not canceled as in monostatic systems [2]. This residual phase may cause defocusing, position errors, and phase errors in the computed images [2], which may compromise the use of the systems for interferometric and tomographic applications.

The generation of high-resolution digital elevation models (DEM) requires the knowledge of relative phases within a few degrees to avoid low-frequency modulation of the DEM in azimuth [3]. In the TanDEM-X mission, synchronization with this level of accuracy was achieved by exchanging radar pulses between the satellites through a direct microwave link [4]. The direct link involved dedicated transmit and receive hardware and a total of six dedicated antennas covering the full solid angle [5].

Besides the need for additional hardware, the incorporation of such direct links may be problematic due to differences in the development schedules of different elements of the constellation, as is the case of companion SAR missions [6]. An alternative solution that does not involves this exchange of pulse could significantly simplify the development of multistatic constellations.

In [7] a full system architecture (MirrorSAR) is envisaged to avoid the demodulation of the radar signals using a different oscillator. The approach consists of having the receivers act like transponders, i.e., re-routing the radar echoes to another element of the constellation (e.g., the transmitter) having access to the oscillator used in the modulation. Although a MirrorSAR architecture requires a direct link between the satellites, not necessarily in the microwaves range, it still keeps the potential for relevant spacecraft simplification by an appropriate design of baselines and the possible removal of complete hardware blocks for demodulation, data storage, downlink, or digital control in the receivers.

Another possibility to could be the estimation of the synchronization phase based on the evaluation of the received data (e.g., autosync). Although demonstrated in space-borne environments [8], [9], it provides estimates with varying quality as a function of the backscattering of the scene, which can only be arguably acceptable as a baseline solution for interferometric SAR missions.

The need to accurately estimated the phase drift of the oscillator is also very important for navigation using a global navigation satellite system (GNSS). This drift affects directly the pseudorange measurements between the GNSS satellite and the GNSS receiver and must be estimated along with the position and velocity in a filter. Exploiting the ability of orbit determination algorithms to provide information on the relative phase drifts between the oscillators of any two elements of a multistatic constellation sounds like a feasible way of approaching the problem.

The capability of high accuracy relative position and timing using GNSS was demonstrated in previous satellite missions. GRACE mission achieved an accuracy of 1 mm compared to a K-Band Ranging System [10]. TanDEM-X achieved an accuracy of the order of 1-2 mm through a-posteriori calibration of the calculated baseline using the processed radar data [11]. Both missions used geodetic grade GPS receivers, capable of receiving two frequencies for correcting the effects of the ionosphere. PRISMA mission demonstrated the capability of achieving sub-decimeter relative positioning precision using a low-cost single-frequency GPS receiver [12].

The proposed solution consists of using a common oscillator for the radar payload and the GNSS receiver, so we can use GNSS data and results from the precise orbit determination to infer the phase noise component in the radar signal. This solution is detailed in the second section. The third section presents a brief error analysis of the proposed solution. A simulation created for evaluating numerically the proposed solution and its results are shown in the fourth section.

2 Proposed solution

Figure 1 shows the block diagram of the GNSS-based solution for the considered problem. The same Ultra Stable Oscillator (USO) is used for generating the radar signal and the reference signal in the GNSS receiver. The natural frequency of the master oscillator is up-converted accordingly for both radar and GNSS receivers.

In the following equations in this section, we denote the upper index $()^{(i)}$ as relating to the GNSS satellite i, the lower indexes $()_u$ and $()_v$ as relating to the receivers in the satellites u and v, and the lower index followed by a comma, as in $()_{u,k}$, as related to the navigation carrier frequency k. Furthermore, we denote the difference between quantities as $()_{uv} = ()_v - ()_u$.

Under the assumption of linearity, the phases of the radar reference signal $\psi_{u,0}$ and of the GNSS receiver $\psi_{u,k}$ are related as follows

$$\psi_{u,0} = \frac{f_0}{f_k} \cdot \psi_{u,k}(t) = \frac{\lambda_k}{\lambda_0} \cdot \psi_{u,k}(t), \qquad (1)$$

where f_0 is the carrier frequency of the radar, f_k is the carrier frequency of the navigation signal k, λ_0 is the carrier wavelength of the radar, and λ_k is the wavelength of the navigation signal k. Eq. (1) suggests that any phase drift in the output of the master oscillator will be replicated in all reference signals derived from it, scaled by the respective up-scaling or down-scaling factors. This assumption remains valid as long as the bandwidth of the reference signals is much smaller than the distance between the harmonics generated in the up-conversion [13].

Let us assume each radar unit u and v incorporates its own GNSS receiver triggered by the radar oscillator as described in Fig. 1. A biased measurement of the distance between the GNSS receiver and the GNSS satellite can be derived from the code delay $P_u^{(i)}$ or the carrier phase measurement $L_u^{(i)}$. The former measurement, based on the detection of the peak, is unambiguous but associated with lesser accuracy. The latter one, based on the measurement of the phase of the peak, is ambiguous but more accurate. Assuming that we can estimate the ambiguity term, a pseudorange can be calculated from the carrier phase measurement as follows

$$P_{Lu,k}^{(i)} = L_{u,k}^{(i)} + \lambda_k \cdot \tilde{A}_{u,k}^{(i)}, \qquad (2)$$

where the term $\lambda_k \cdot \tilde{A}_u^{(i)}$ corresponds to an estimate of the true ambiguity $\lambda_k \cdot A_u^{(i)}$. For the remainder of this paper, we consider the pseudorange shall be obtained from the carrier phase measurement as shown in Eq. (2) since it provides a much higher accuracy assuming that the ambiguity term can be accurately determined.

Assuming that the spacecrafts are close enough so that the ionospheric delay is the same for them, and thus cancel out when taking the difference between the pseudorange measurements, the relationship between the differences of the pseudoranges $P_{Luv,k}^{(i)}$ and the clock biases expressed in time δt_{uv} is given by [14]

$$P_{Luv,k}^{(i)} = \rho_{uv}^{(i)} + c \cdot \delta t_{uv} + \epsilon, \qquad (3)$$

where $\rho_{uv}^{(i)}$ is the difference between the distances from receivers v and u to the i-th navigation satellite, respectively, c is the velocity of propagation of the navigation signals, and ϵ is the measurement error, which includes systematic and noise-like contributions as, for example, thermal noise in the receivers and the ambiguity estimation errors. Isolating the clock bias term we can identify the relationship between the navigation data and the clock synchronisation solution as follows

$$c \cdot \delta t_{uv} = \frac{\lambda_0}{2\pi} \cdot \psi_{uv,0} = P_{Luv,k}^{(i)} - \rho_{uv}^{(i)} - \epsilon, \qquad (4)$$

An estimator of the clock synchronization solution using a weighted average over all navigation satellites in sight (i.e., N) and all the $n_\lambda^{(i)}$ received GNSS frequencies can be straightforwardly derived as

$$\tilde{\psi}_{uv,0} = \frac{2\pi}{\lambda_0} \cdot \sum_{i=1}^{N} \sum_{k=1}^{n_\lambda^{(i)}} \alpha_i \cdot \frac{P_{Luv,k}^{(i)} - \tilde{\rho}_{uv}^{(i)}}{n_\lambda^{(i)}}, \qquad (5)$$

where $\tilde{\rho}_{uv}^{(i)}$ is the estimated value of $\rho_{uv}^{(i)}$ as provided by POD (e.g., through direct estimation or interpolation), and α_i are the weights for the signal from each navigation satellite according to its quality (e.g., signal-to-noise ratio). Eq. (5) provides an unbiased estimation under the assumption that ϵ is a zero-mean process, and no relevant biases are introduced in the baseline determination process. As hinted earlier, the term in the summation contains systematic error components that may bias the resulting estimates if not properly removed.

Assuming the measurements are statistically independent Gaussian processes, the value of α_i which minimizes the variance of the estimator is given by

$$\alpha_i = \frac{\sigma_i^{-2}}{\sum_{k=1}^{N} \sigma_k^{-2}}. \qquad (6)$$

where the σ_i correspond to the standard deviation of the measurement related to GNSS satellite i (e.g., of the residuals of the POD). Sensible assumptions for the derivation of the estimator performance are i) the measurements were calibrated, eliminating major systematic components and ii) the measurement is dominated by thermal noise in the receiver. Under these circumstances, the σ_i can be expressed as a function of the carrier-to-noise ratio $(c/n_0)_i$ as follows

$$\sigma_i \approx \sqrt{\frac{B_{\text{L-CA}}}{(c/n_0)_i}}, \qquad (7)$$
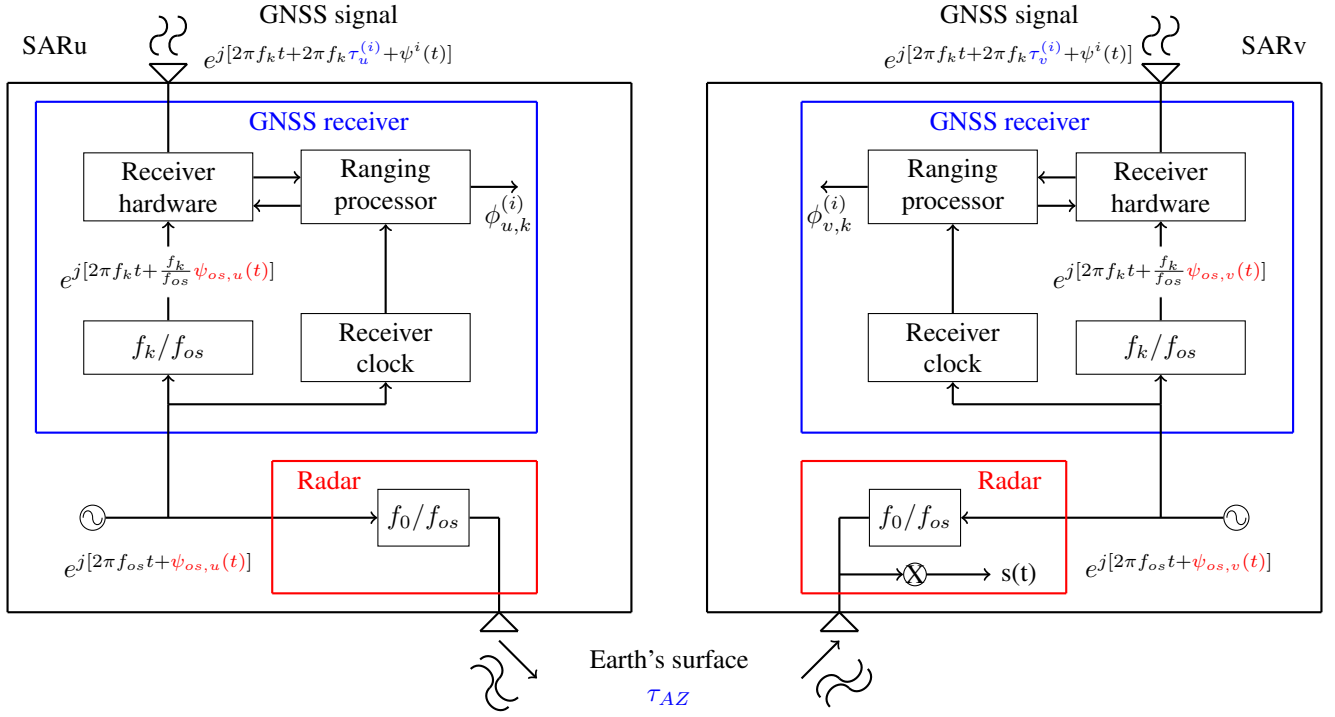
Figure 1 Proposed hardware configuration for radar phase synchronization based on GNSS, also used as basis for the analysis. In this figure, $\tau^{(i)}$ are the delays from GNSS satellite to the SAR satellites. The terms $A_{()}^{(i)}$ accounts for the ambiguity of the carrier phase measurements.

where $B_{\mathrm{L-CA}}$ is the so-called tracking bandwidth of the GNSS receiver for a Phase Lock Loop discriminator [15]. Substituting (7) into (6) we get

$$\alpha_i \approx \frac{(\mathrm{c}/n_0)_i}{\sum_{k=1}^N (\mathrm{c}/n_0)_k}, \tag{8}$$

where the (c/n_0) values provided by the GNSS receiver can be used.

Note that the phase noise affecting the radar measurements is the phase differences between the transmitter and receiver oscillators evaluated at times delayed by τ the two-way travel time of the radar signals. This lag, in the order of milliseconds, is well beyond the inverse of the bandwidth of the oscillators phase noise, which allows us to approximate

$$\psi_v(t - \tau) - \psi_u(t) \approx \psi_v(t) - \psi_u(t) \quad . \tag{9}$$

Assuming Eq. (9) is valid, the solution of the oscillator phase noise provided by the navigation solution can be effectively used for the calibration of the phase reference of the radar data.

3 Error analysis

The previous section provides a simplified model for the estimation of the oscillator synchronization phase based

on the exploitation of GNSS data. As already hinted, a more realistic approach needs to incorporate several systematic components that contribute to the error in the pseudoranges. A more accurate description of the difference between the carrier phase measurements of receivers u and v is given by [14]

$$L_{uv,k}^{(i)}(t) = \rho_{uv}^{(i)}(t) + \mathrm{c} \cdot \delta t_{uv}(t) - \left(\frac{\lambda_k}{\lambda_1}\right)^2 \cdot I_{uv}^{(i)}(t) - \\ \lambda_k \cdot A_{uv,k}^{(i)} + M_{uv,k}^{(i)}(t) + \epsilon_{uv,k}^{(i)}(t), \tag{10}$$

in which $A_{uv}^{(i)}$ is the difference between the ambiguities, $M_{uv}^{(i)}(t)$ describes other systematic error components including multipath, cross-talk, tracking channel bias and phase wind-up, and $\epsilon_{uv}^{(i)}(t)$ is a thermal noise process. Eq. (10) is valid under the assumption that the measurement times between the two satellites are sampled at approximately the same epoch and the positioning and timing errors due to temporal misalignment are negligible compared to the other error sources. A similar condition is required for precise baseline determination.

A further elaboration of the system model suggests that the incorporation of independent phase noise realizations occurring in the up-conversion stages of the radar and navigation receiver electronics, which may be in principle different for each navigation frequency. Under these circum-

stances, we can relate the phase differences at radar and navigation carriers between the two satellites as follows

$$\psi_{uv,0}(t) = \frac{\lambda_k}{\lambda_0} \cdot [\psi_{uv,k}(t) + \Delta\psi_{uv,k}(t)] , \qquad (11)$$

where $\Delta\psi_{uv,k}$ denotes the additional phase noise introduced in the up-conversion stages for the radar and navigation carriers at the level of the latter.

The error in the estimation of the differential phase at the radar carrier can be derived after combining (5), (10), (2), and (11) as follows

$$\delta\psi_{uv,0}(t) = \sum_{i=1}^{N} \sum_{k=1}^{n_\lambda^{(i)}} \frac{2\pi \cdot \alpha_i}{\lambda_0 \cdot n_\lambda^{(i)}} \cdot \left\{ \frac{\lambda_k}{2\pi} \cdot \Delta\psi_{uv,k}(t) + \epsilon_{uv,k}^{(i)}(t) \right. $$
$$+ \left[\rho_{uv}^{(i)}(t) - \tilde{\rho}_{uv}^{(i)}(t) \right] + \lambda_k \cdot \left(A_{uv,k}^{(i)} - \tilde{A}_{uv,k}^{(i)} \right)$$
$$\left. + \left[M_{uv,k}^{(i)}(t) - \left(\frac{\lambda_k}{\lambda_1} \right)^2 \cdot \left(I_{uv}^{(i)}(t) - \tilde{I}_{uv}^{(i)}(t) \right) \right] \right\} .$$
$$(12)$$

Each term of the previous expression within curly brackets describes an error component of the POD-based estimation of the radar synchronization phase, averaged over all tracked GNSS signals and scaled by the corresponding radar wavelength. These components are summarized in the bullets below:

- Up-conversion error for both the radar and navigation carriers;

- Receiver noise;

- Baseline determination error arising from POD;

- Ambiguity resolution error, which is expected to remain constant over a continuous tracking period for each GNSS satellite;

- A mismodeling term including error in the estimation of ionospheric delay difference between satellites, multipath, phase bias on the receiver tracking channel, phase wind up and other systematic errors.

Since the error components are proportional to the inverse of the radar wavelength, the estimation error is expected to increase for higher radar frequencies.

4 System example

Figure 2 shows the data flow and the major components of the simulation used for testing the concept explained in the previous sections. A bistatic SAR system composed of a transmitter and receiver flying in close formation and possessing the suggested hardware configuration has been considered. The navigation antennas of the radar satellites have direct visibility with 9 GPS satellites. The orbits of all satellites are propagated using the open-source software GMAT distributed by NASA. The software allows for numerical integration of the orbit using an accurate gravitational model and including drag and third bodies attraction. The errors in the position and velocity of the radar

satellites coming from the precise orbit determination have been simulated by introducing an absolute bias in the initial state of the satellites and propagating the orbit. Two cases were simulated: One in which only error in the position vector is introduced, and another in which errors in the position and velocity vector are introduced.

After propagating the orbits, the ranges between the radar satellites and the GNSS satellites in view at a minimum elevation of 10 degrees are calculated. The navigation raw data are simulated by adding the following error components to the expected code signal: ionospheric delay, initial clock bias, thermal noise, and clock drift. The phase drift realization corresponds to a real measurement taken through the synchronization link of TanDEM-X operated at a frequency of 3 kHz.

The simulations assume a single frequency GNSS receiver. The noise figure used in the simulations is in line with the Phoenix GNSS receiver from GSOC/DLR [16]. The error figures are in the sub-decimeter level, in line with the results from PRISMA mission, which used a single-frequency GNSS receiver.

The phase difference between the clocks is estimated using equation (5). In case the receiver was capable of receiving two frequencies, the final results would improve by a factor of $\sqrt{2}$ due to the availability of a second independent measurement, in addition to the improved accuracy due to a more accurate orbit determination.

Table 1 shows the simulation parameters and baseline errors concerning the specific cases shown in the next section. The baseline errors are expressed in Hill's frame.

Table 1 Simulation parameters

Parameter	Value
GNSS data sampling rate	1 MHz
GNSS signal frequency	1575.42 MHz
Radar payload frequency	9656 MHz
Pseudorange standard deviation	0.0005 m
GNSS position bias	2 m
Ionospheric range error	10 m
Radial baseline error	8.248 mm
Along-track baseline error	1.177 mm
Across-track baseline error	0.767 mm
Radial baseline velocity error	0.0057 mm/s
Along-track baseline velocity error	-0.0077 mm/s
Across-track baseline velocity error	-0.0027 mm/s

The noise figure from the carrier phase measurements is used. The implicit assumption is that the integer ambiguity factor is known from the precise orbit determination process. The noise figures of the code delay measurements are much higher and are expected to worsen between one and two orders of magnitude the accuracy of the estimates.

Below the results of the phase estimation for two cases: one in which the baseline velocity error is zero and the other where there is some considerable baseline velocity error. For both cases, the baseline errors are the ones reported in table 1.

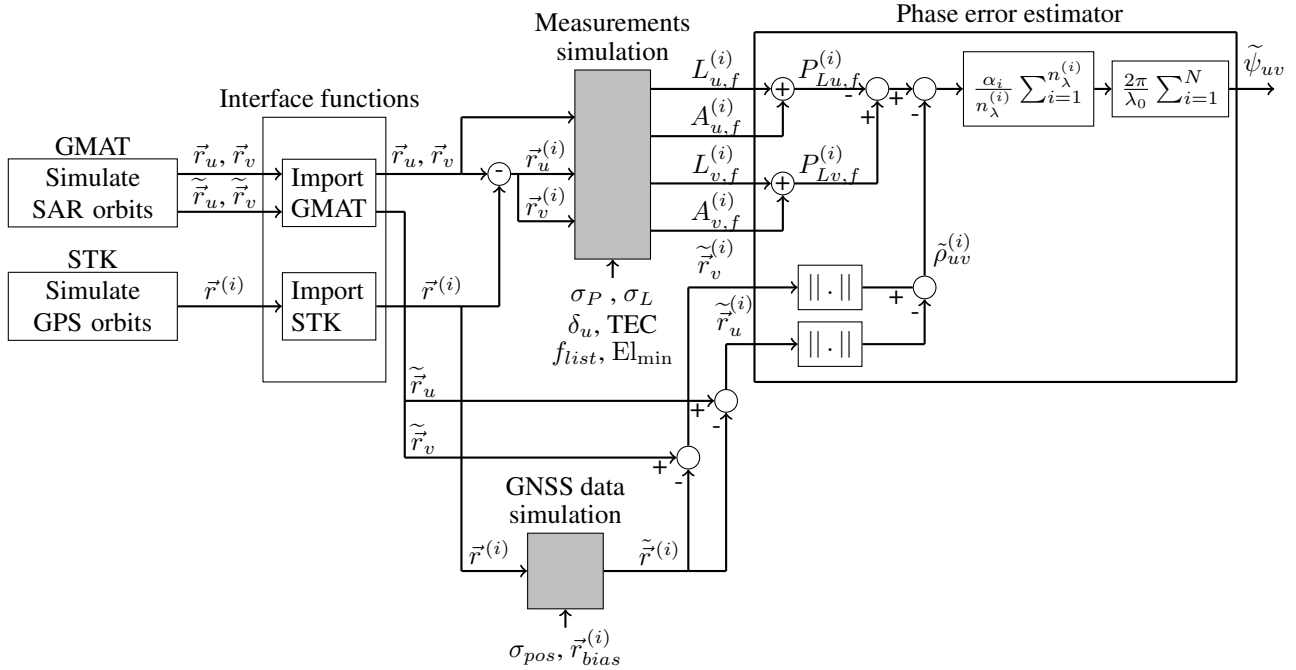Figure 3 shows the results of the simulation for the case

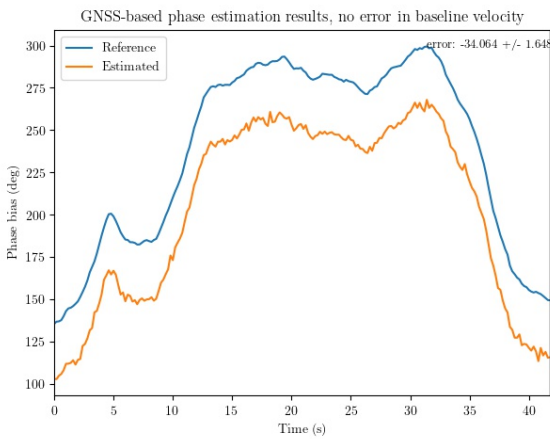**Figure 2** Simulation framework used to test the proposed POD-based phase synchronization.

Figure 3 Simulated phase drift data and estimation results from multiple GNSS data. Case with error only in the baseline vector
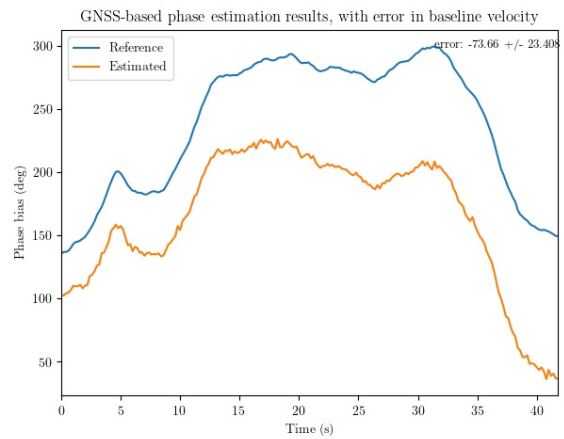

Figure 4 Simulated phase drift data and estimation results from multiple GNSS data. Case with initial errors in the baseline and baseline velocity vectors

without a baseline velocity error. We can see that the suggested approach provides a good estimate with a standard deviation of less than two degrees. The constant bias of around 34 degrees corresponds to the bias in the baseline estimates. Although the error was introduced only in the initial baseline, it remains approximately constant during the simulation time span. Such constant bias in the phase noise can be typically estimated with very high accuracy by an appropriate evaluation of the radar data.

Figures 4 and 5 show the results for the simulation including a baseline velocity error. Figure 5 demonstrates that an error in the baseline velocity is interpreted as a clock frequency offset by the estimation algorithm. Such an error can heavily degrade the accuracy of the radar images, introducing geolocation errors and interferometric phase

ramps [17]. The proposed solution, therefore, depends on a very accurate estimation of the relative baseline velocity. In case the error in the estimation of relative baseline velocity is not negligible, an approach based on the SAR data processing such as the ones described in [18] could be used to potentially eliminate the phase ramp.

Note that there are other error components not considered in the estimation that are expected to affect the final accuracy result. In particular, the multipath effects could degrade considerably the precision and accuracy of the solution. The unmodeled sources which do not remain constant during the time span of the radar integration time must be carefully examined. In case the error remains constant, it will cause a constant phase shift which may be compensated by appropriate processing.
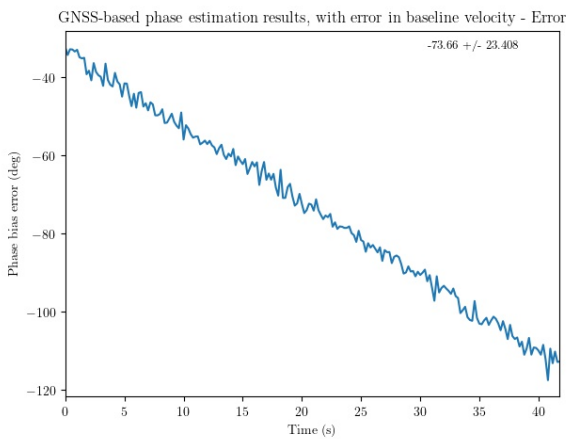
Figure 5 Error in the estimation from multiple GNSS data. Case with initial errors in the baseline and baseline velocity vectors

5 Conclusions

In conclusion, the technique here presented offers an alternative low-cost simple solution for the phase synchronization in bistatic or multistatic constellations. It also indicates that a sufficiently good performance could be obtained from a low-cost GNSS receiver. The solution relies on very precise relative navigation data. It assumes that the precision is in the sub-decimeter level in relative precision and negligible in relative velocity. For further evaluation of the idea, a more detailed error analysis is necessary, including a solution for compensating those which introduce fast varying biases in the raw measurements.

6 Literature

[1] Krieger, G.: Fiedler, H.: Moreira, M.: Bi-and multistatic SAR: potentials and challenges. In Proc. EUSAR, vol. 34, pp. 365-370. 2004.

[2] Krieger, G.: Younis, M.: Impact of oscillator noise in bistatic and multistatic SAR. IEEE Geoscience and Remote Sensing Letters 3, no. 3 (2006): 424-428.

[3] Krieger, G.: Fiedler, H.: Hajnsek, I.: Eineder, M.: Werner, M.: Moreira, A.: TanDEM-X: mission concept and performance analysis. In International Geoscience and Remote Sensing Symposium, vol. 7, p. 4890. 2005.

[4] Braubach, H.: Voelker, M.: Method for drift compensation with radar measurements with the aid of reference radar signals. U.S. Patent 7,209,072, issued April 24, 2007.

[5] Krieger, G.: Moreira, A.: Fiedler, H.: Hajnsek, I.: Werner, M.: Younis, M.: Zink, M.: TanDEM-X: A satellite formation for high-resolution SAR interferometry. IEEE Transactions on Geoscience and Remote Sensing 45, no. 11 (2007): 3317-3341.

[6] Rodriguez-Cassola, M.: Prats-Iraola, Pau.: Zonno, M.: Nannini, M.: López-Dekker, P.: Carnicero-Dominguez, B.: Rommen, B.: Moreira, A.: End-to-end performance analysis of companion SAR missions. In 2017 IEEE International Geoscience and Remote Sensing Symposium (IGARSS), pp. 153-156. IEEE, 2017.

[7] Krieger, G.: Zonno, M.: Mittermayer, J.: Moreira, A.: Huber, S.: Rodriguez-Cassola, M.: Mirrorsar: A fractionated space transponder concept for the implementation of low-cost multistatic sar missions. In EUSAR 2018; 12th European Conference on Synthetic Aperture Radar. Aachen, Germany: pp. 1–6. VDE, Jun. 2018.

[8] Rodriguez-Cassola, M.: Prats, P.: Schulze, D.: Tous-Ramón, N.: Stein- brecher, U.: Marotti, L.: Nanninni, M.: Younis, M.: Zink, M.: Reigber, A.: López-Dekker, P.: Krieger, G.: Moreira, A.: First bistatic spaceborne SAR experiments with tanDEM-X. IEEE Geosci. Remote Sens. Lett., vol. 7, no. 1, pp. 108–112, Jan. 2012.

[9] Rodriguez-Cassola, M.: Bistatic synthetic aperture radar data processing. Ph.D. dissertation, DLR Technical Report, 2012.

[10] Kroes, R.: Montenbruck, O.: Bertiger, W.: Visser, P.: Precise GRACE baseline determination using GPS. GPS Solutions 9, no. 1 (2005): 21-31.

[11] González, J. H.: Mohan, J. W. A.: Bachmann, M.: Krieger, G.: Zink, M.: Schrank, D.: Schwerdt, M.: Bistatic system and baseline calibration in TanDEM-X to ensure the global digital elevation model quality. ISPRS Journal of Photogrammetry and Remote Sensing 73 (2012): 3-11.

[12] Ardaens, J. S.: D'Amico, S.: Montenbruck, O.: Flight results from the PRISMA GPS-based navigation. In 5th ESA Workshop on Satellite Navigation Technologies, NAVITEC, pp. 8-10. 2010.

[13] Pozar, D. M.: Microwave engineering. Wiley (2012).

[14] Kroes, R.: Precise relative positioning of formation flying spacecraft using gps. Ph.D. dissertation, Delft University of Technology, Apr. 2006.

[15] Groves, P. D.: Principles of GNSS, inertial, and multisensor integrated navigation systems. Artech house, 2013.

[16] Phoenix GPS Data Sheet, Issue 1.1, January 2007.

[17] Rodriguez-Cassola, M.: Prats, P.: Schulze, D.: Tous-Ramon, N.: Steinbrecher, U.: Marotti, L.: Nannini, M.: Younis, M.: López-Dekker, P.: Zink, M.: and Reigber, A.: First bistatic spaceborne SAR experiments with TanDEM-X. IEEE Geoscience and Remote Sensing Letters 9, no. 1 (2011): 33-37.

[18] Rodriguez-Cassola, M.: Prats, P.: López-Dekker, P.: Reigber, A.: Krieger, G.: Moreira, A.: Autonomous time and phase calibration of spaceborne bistatic SAR systems. In EUSAR 2014; 10th European Conference on Synthetic Aperture Radar, pp. 1-4.